Analytical Methods

Accepted Manuscript

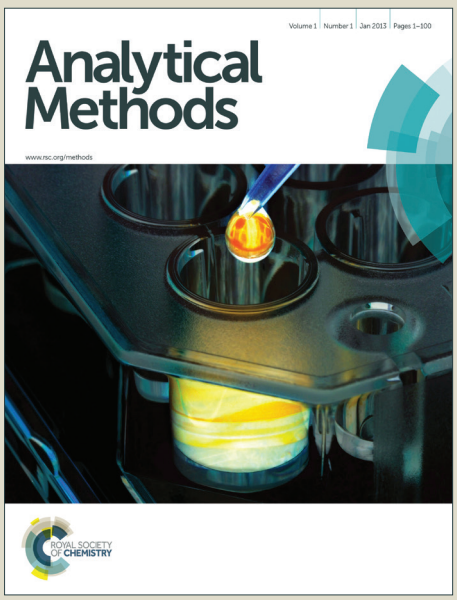

ROYAL SOCIETY OF CHEMISTRY

www.rsc.org/methods

A dynamic anti-aggregation sensing method using unmodified gold nanoparticles(AuNPs) for rapid detection of Hg^{2+}.

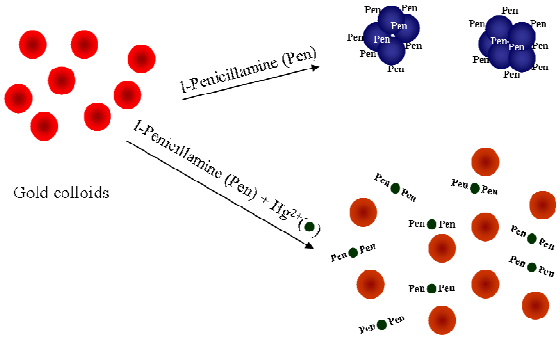

Development of a Gold Nanoparticle Based Anti-aggregation Method for Rapid Detection of Mercury(II) in Aqueous Solutions

Genin Gary Huang[*]*, Yen-Ting Chen, and Yu-Rong Lin*

Department of Medicinal and Applied Chemistry, Kaohsiung Medical University,

Kaohsiung, 807, Taiwan

*To whom correspondence should be addressed.

E-mail: genin@kmu.edu.tw

Phone: +886-7-312-1101 ext. 2810 Fax: +886-7-312-5339

Abstract

This study proposes a dynamic anti-aggregation sensing method for detecting mercury(II) ions in aqueous solutions. The proposed method is based on the aggregation of gold nanoparticles (AuNPs) in the presence of an aggregation agent inhibited by Hg^{2+} because of high affinities between the mercury(II) ions and the aggregation agents. The aggregation agents tend to coordinate with Hg^{2+} rather than be absorbed on the AuNP surfaces, causing the size and axial ratio of the retained gold nanocolloids to be mostly unaffected. Because the extinction maxima are affected by the size, axial ratio, and morphologies of gold nanoaggregates, mercury(II) ions can be detected by comparing the extinction spectra of gold nanocolloids in both the presence and absence of mercury(II) ions. The proposed sensing method demonstrates the advantage of requiring no surface modification of AuNPs, and enables rapid detection with acceptable sensitivity and selectivity. Under optimized conditions, the detection limit toward Hg^{2+} is ca. 25 nM.

Introduction

The mercury(II) ion, one of the most stable and abundant forms of mercury, can cause severe damage to humans and other living beings.[1-4] Because of its medical and ecosystem relevance, the detection of Hg^{2+} has been investigated extensively.[5] Conventional atomic spectroscopic techniques, including atomic absorption spectroscopy,[5-11], atomic emission spectroscopy,[5,6,12-16] and atomic fluorescence spectroscopy,[17-20] have been commonly applied in detecting Hg^{2+}. In addition, inductive coupled plasma mass spectrometry[6,21,22] and various electrochemical methods have been widely used in analyzing Hg^{2+} levels.[23-25] The sensitivity, precision, and reliability of these analytical methods are appropriate for detecting Hg^{2+}. However, the sophisticated instrumentation and relatively complex sample pretreatment procedures involved in these methods have limited practical applications.

Gold nanoparticle (AuNP)-based colorimetric sensing methods provided an alternative for detecting mercury(II) ions. The localized surface plasmon resonance (LSPR)[26,27] effect of appropriately sized nanosized AuNPs extinct visible radiation, and the extinction coefficients are generally three orders higher than those of fluorescent dye molecules.[28] Furthermore, the extinction maximum of AuNPs is primarily determined according to the size and aspect ratio of nanoparticles.[29,30] These characteristics enable distinguishing color variations by using the naked eye, thereby increasing the feasibility of using AuNP-based colorimetric sensing methods in on-site and real-time detection.[29,31] Regarding the AuNP-based colorimetric sensing methods for detecting mercury(II) ions, the modification of functional molecules on the surfaces of the nanoparticles is a frequently used protocol. During the detection of Hg^{2+}, the dispersed nanoparticles are attracted and aggregated by forming mercury complexes between Hg^{2+} and chelators modified on different AuNPs. Observing the

extinction maximum shifts caused by the changes in aggregate size enables monitoring the mercury(II) ion concentration.[28,31-42] Once fluorescent molecules or quantum dots are modified, the energy transfer between AuNPs and light emitters induced by Hg^{2+} can "turn-on" or "turn-off" the fluorescence and emittance, which can be applied in tracing the concentration levels of Hg^{2+}.[43-47] Although the surface modification strategy requires no intricate instrumentation, the modification procedures still increase the complexity and the analysis time. Recently, a reversed AuNP-based Hg^{2+} detection strategy called "anti-aggregation" was proposed.[48-50] The aggregation of AuNPs induced by aggregation agents can be prohibited by forming metal complexes between Hg^{2+} and aggregation agents in the presence of Hg^{2+}. Although the anti-aggregation strategy eliminates the complex surface modification processes, more than 30 min of incubation time is still required.[43-47] Therefore, this study proposes a novel anti-aggregation AuNP-based colorimetric sensing method for detecting Hg^{2+}. Using a thiol-containing amino acid molecule l-penicillamine as the aggregation agent enables the aggregation of AuNPs to be impeded by the presence of Hg^{2+}. Compared with other sensing methods, the proposed anti-aggregation strategy enables observing the results directly by using the naked eye, and the surface modification of AuNPs is unnecessary. Additionally, the sensing procedure can be accomplished in 2 min, thereby substantially increasing the efficiency of the proposed sensing method.

Experimental Section

Materials

Chloroauric acid, trisodium citrate, nitric acid, sodium acetate, sodium phosphate, sodium hydroxide, l-cysteine methyl ester hydrochloride, l-glutathione, l-penicillamine, l-methionine, tartaric acid, boric acid, mercury(II) chloride, copper(II) chloride, lead(II) chloride, sodium(I) chloride, nickel(II) chloride, cobalt(II) chloride,

calcium(II) chloride, ferric(III) chloride, and zinc(II) chloride were purchased from Alfa Aesar; l-cysteine, dl-homocysteine, and tris(hydroxymethyl) aminomethane (TRIS) were obtained from Sigma Aldrich. All of the chemicals are reagent grade and used as received without further purification. Deionized Milli-Q water (Simplicity^{TM}, Millipore) was also used throughout the study.

Preparation of the Gold Nanoparticle Colloidal Solution

The citrate-reduced AuNP colloidal solution used in this study was prepared according to literature previous study.[51] In brief, 500 mL of 1.4 mM $HAuCl_{4(aq)}$ was refluxed to a boil during vigorous stirring. A total of 50 mL of 1% (w/v) trisodium citrate aqueous solution was added at the boiling point, and the solution was maintained at the boiling point for 1 h. The extinction maximum of the prepared gold nanocolloids was 525 nm, and the average size of the AuNPs was approximately 20 nm.[52,53]

Extinction Spectra Measurements

For measuring Hg^{2+}, 1500 μL of buffer solutions were mixed with 300 μL of aggregation agent solutions and 600 μL of Hg^{2+} solutions prior to the addition of 600 μL of gold colloidal solutions. Parallel experiments were conducted to compare the aggregation behaviors of AuNPs without the disturbance of the mercury ions. Different incubation time was examined to find the optimized incubation time. The results indicated that AuNPs aggregated right after mixing with aggregation agents and the aggregation bands approached to absorption maxima after 2min of incubation. On the other hand, the aggregation of AuNPs was suppressed in the presence of AuNPs and no signs of aggregation were observed after 6min of incubation. Therefore, each measurement was performed after 2 min of incubation (See electronic supplementary information). All of the extinction spectra in this study were measured using a Thermo scientific Genesys 10S Bio UV/Visible spectrometer with a 1 nm

resolution. The wavelength range from 400 to 1000 nm was recorded. The path length of the UV-Vis cell was 1 cm. Transmission electron microscopy (TEM) was employed using a JEM-2000EXII microscope (Jeol) with an accelerating voltage of 100 kV, to observe the aggregation of AuNPs in the presence and absence of Hg^{2+}. Scheme 1 depicts the proposed sensing scheme. The extinction of AuNPs caused by LSPR was critically affected by the size, aspect ratio, and morphology of the nanoparticles.[29] Regarding AuNPs from 6 to 20 nm in size, the extinction was approximately 525 nm.[52,53] A new aggregation band was observed after the addition of aggregation agents because the sizes of the gold nanoaggregates increased. As described in the previous section, the aggregation of AuNPs is suppressed in the presence of Hg^{2+} ions because the mercury(II) ions have high affinities with aggregation agents; thus, the size and morphologies of gold nanocolloids can be retained and mostly unaffected. The ability to suppress AuNP aggregation is related to the concentration of mercury(II) ions. Identifying mercury(II) ions can be achieved by comparing the extinction spectra of gold nanocolloids in the presence and absence of Hg^{2+}.

Results and Discussion

Detecting Hg^{2+} by Using Different Aggregation Agents Under Various Chloride Concentrations

The AuNPs prepared using reductions of chloroauric acid were dispersed in aqueous solutions because of the negative surface zeta potential caused by the adsorbed citrate anions and their analogs after citrate oxidation.[54] The aggregation of gold nanocolloids can generally be induced by adding molecules with thiols and amines, which interact strongly with gold surfaces.[55] Therefore, six amino acid analog-bearing thiol groups were examined to determine their effectiveness as adequate aggregation agents for detecting Hg^{2+}. The structures of the aggregation

agents examined in this study are given in the electronic supplementary information. However, adding halide ions accelerates the aggregation of colloids.[56,57] Therefore, the anti-aggregation capability of Hg^{2+} can be different under different degrees of AuNPs aggregation caused by different concentrations of halide ions. To investigate the combined effects of aggregation agents and halide ions, mercury(II) ions were detected using different aggregation agents in various concentrations of chloride ions. In addition, parallel experiments were conducted to observe the aggregation behaviors of six aggregation agents without disturbing by the mercury ions. Figure 1A shows a plot of the measured extinction spectra of as-prepared gold nanocolloids in the presence and absence of 1 μM Hg^{2+} accompanied by different aggregation agents and chloride ion concentrations. The extinction ratio at 525 and 750 nm under different conditions were calculated, and the results are plotted in Figure 1B. As the figures indicate, adding six aggregation agents induced the aggregation of gold nanocolloids, and the aggregation became more critical as the concentration of chloride ions increased, except for l-penicillamine. In the presence of mercury(II) ions, the extinction spectra showed that the aggregation of gold nanocolloids was inhibited significantly when l-methionine or l-penicillamine was used as the aggregation agent, whereas the other four aggregation agents exhibited only minor variations. The results suggested that once l-penicillamine chelate with Hg^{2+}, they are no more capable of inducing AuNPs aggregation since the thiol groups, carboxylic groups, and amino groups of l-penicillamine are all participated in chelation and become no more available in inducing AuNPs aggregation. As the concentration of chloride ions increased, the anti-aggregation effect induced by mercury(II) ions became imperceptible when l-methionine was used as the aggregation agent whereas the anti-aggregation effect was mostly unaffected when l-penicillamine was used as the aggregation agent. Figure 2(A) shows the TEM images of AuNP aggregates induced

by l-penicillamine, and Figure 2(B) shows the same nanocolloids in the presence of l-penicillamine and Hg^{2+}. Clearly, the addition of Hg^{2+} was significant to keep the AuNPs dispersed. Therefore, l-penicillamine was the most suitable aggregation agent among the six examined agents. The ratio values of un-aggregated LSPR bands to aggregation bands suggested that the most significant difference was observed as the chloride ion concentration reached 10 mM.

Optimizing the Aggregation Agent Concentration

The sensing scheme of this study is based on dynamic anti-aggregation of AuNPs in the presence of mercury(II) ions. Because the aggregation agents chelated with Hg^{2+}, the aggregation agents have no more active sites to bind AuNPs. The anti-aggregation capability of mercury(II) ions was different as the aggregation agent varied because of the distinct stability constants of Hg^{2+}-aggregation agent complexes. Similarly, the equilibrium of the sensing system was also affected by the concentration of the aggregation agent. To understand the effect of the aggregation agent concentration further, mercury(II) ions were detected in different concentrations of l-penicillamine while the sensing system consisted of 10 mM chloride ions. The band ratio values at 525 and 750 nm under different aggregation agent concentrations were obtained, and the results are plotted in Figure 3. When the concentration of the aggregation agent is higher than 3.5 μM, the presence of Hg^{2+} no longer interfered with the aggregation of the AuNPs, because the free aggregation agent remained, later forming mercury complexes. As the concentration of l-penicillamine was reduced, the presence of Hg^{2+} suppressed the aggregation of the gold nanocolloids and the results showed the most significant difference between the systems with Hg^{2+} and those without Hg^{2+} was the concentration of the aggregation agent at 2 μM.

pH Effects in Detecting Mercury(II) Ions

The aggregation agent used in this study is l-penicillamine, which has pK_a values of 2.44, 7.97, and 10.46, corresponding to –COOH, $–NH_2$, and –SH, respectively.[58,59] The chelating ability of l-penicillamine is therefore affected by the pH of the sensing system. Meanwhile, the stability of AuNPs are also affected by the pH since the negative surface zeta potential of citrated reduced AuNPs is varied as the pH changed, which implies the anti-aggregation ability of Hg^{2+} is consequently influenced by the pH. However, the aggregation of AuNPs induced by penicillamine was reported to be pH dependent.[60] To understand how l-penicillamine induced AuNPs aggregation were affected by the pH of the system in the presence and absence of Hg^{2+}, extinction spectra of gold nanocolloids in the presence of l-penicillamine and Hg^{2+} under different pHs were measured. For ease of comparison, the spectra of gold nanocolloids in the absence of Hg^{2+} were also measured, and all of the band ratio values at 525 and 750 nm under different conditions were calculated, and the results are plotted in Figure 4. In the absence of Hg^{2+}, substantial aggregation of AuNPs induced by l-penicillamine was observed when the pH of the gold colloidal solution was less than 3. By contrast, the aggregation of AuNPs induced by l-penicillamine was suppressed in the presence of Hg^{2+}, unless the pH was under conditions that were more acidic (pH of approximately 2). By comparing the band ratio values at 525 and 750 nm before and after the addition of Hg^{2+}, it was determined that the most appropriate pH of the sensing system is 2.4.

Optimizing the Buffer Solutions

In the experimental section, we explain that the sensing system consisted of buffer species to resist the pH variation. The buffer species that were used are generally capable of chelating with metal ions so that the buffer species also act as the auxiliary chelating agents; thus, the anti-aggregation of AuNPs induced by Hg^{2+} is affected. To determine the effects of the buffer species used for detecting Hg^{2+}, six

buffer species, citrate, tartrate, borate, phosphate, acetate, and TRIS, were examined, and the band ratio values at 525 and 750 nm, obtained using different buffer species, are plotted in Figure 5A. The ratio values between the gold nanocolloids in the presence of Hg^{2+} and those in the absence of Hg^{2+} showed less variation when tartrate or TRIS was used as the buffer species. By comparison, the other four buffer species presented differences that were more significant. The logarithmic values of Hg^{2+} complex formation constants with citric acid, phosphate, and acetic acid, are 10.9, 9.5, and 8.4, respectively.[61,62] The similar formation constants with Hg^{2+} constitute the probable reason why the band ratio values between the gold nanocolloids with Hg^{2+} and those without Hg^{2+} were similar when these four species were used to prepare the buffer solutions. To simplify the system as much as possible, citrate was used to prepare the buffer solution because the AuNPs used in this study were prepared by reducing chloroauric acid with citrate. Because the mercury(II) ion detection ability of the proposed sensing system is affected by the concentration of the aggregation agent, the concentration of the buffer solution (the auxiliary chelating agent) changed the anti-aggregation behaviors of the gold nanocolloids in the presence of aggregation agents and Hg^{2+}. A plot of the band ratio values from using different citrate buffer concentrations in the presence and absence of Hg^{2+} is shown in Figure 5B. Figure 5B shows that the aggregation of AuNPs induced by l-penicillamine without the addition of Hg^{2+} was relatively mild when the concentration of the citrate buffer was 2.5 mM. Because the pH of the solution was set at 2.4, the -COOH groups of citrate consisted of both protonated and deprotonated forms, which reduced the stability of AuNPs by forming hydrogen bonds between citrate groups of different gold nanocolloids similar to penicillamine-induced AuNPs aggregation.[60] Consequently, the aggregation of gold nanocolloids became critical when the concentration of citrate was greater than 5 mM. In the presence of Hg^{2+}, all of the AuNPs were dispersed until the concentration of

citrate exceeded 15 mM. These results indicate that the citrate ions were factors in probing Hg^{2+}. Under acidic conditions, the citrate ions promoted the aggregation of gold nanocolloids, and the sensitivity toward Hg^{2+} was thereby affected.

Effects of the Gold Nanoparticle Concentrations

The proposed sensing method is based on the dynamic equilibriums among gold nanocolloids, aggregation agents, and Hg^{2+} ions. The experimental results showed that the detection of Hg^{2+} was affected by the origins and concentrations of the aggregation agents. Similarly, the variations in gold nanocolloid particle concentration also agitated the dynamic equilibrium. The size of the AuNPs prepared in this study was approximately 20 nm with the extinction maximum at 525 nm, which corresponds to the molar absorptivity (ε) of $8.78\pm0.06 \times 10^8$. The particle concentration can be estimated at 2.85 nM.[29,30,52,53] To determine how the gold nanocolloid particle concentration affects the equilibrium, different particle concentrations of gold nanocolloidal solutions were prepared and used for detecting Hg^{2+}. The band ratio values at 525 and 750 nm with different particle concentrations in the presence and absence of Hg^{2+} were examined, and the results are plotted in Figure 6. Because the presence of Hg^{2+} cannot induce the anti-aggregation of AuNPs in a low gold nanocolloid particle concentration (< 1.4 nM), the band ratio values showed no difference between the AuNP solutions with and without Hg^{2+}. The dynamic equilibrium was shifted to the aggregation even in the presence of Hg^{2+} because the relative concentration of l-penicillamine was twice that of the origin, thus revealing the similar tendencies of varying the concentration of l-penicillamine, as shown in Figure 3. Likewise, the aggregation of gold nanocolloids tended to be insignificant as the particle concentration of gold nanocolloids increased to 5.70 nM, because the aggregation agent became relatively limited under this condition.

Linearity, Detection Limit, and Selectivity in Detecting Hg^{2+}

After the sensing system was optimized by adjusting the conditions of the aggregation agents, pH, buffer solutions, and particle concentrations of the gold nanocolloids, the sensitivity of the optimal sensing system toward the detection of Hg^{2+} was determined by examining different concentrations of Hg^{2+} (Extinction spectra of AuNPs in the presence of different concentrations of Hg^{2+} were shown in the electronic supplementary information). The band ratio values at 525 and 750 nm in the presence of different concentrations of Hg^{2+} were obtained, and the results are plotted in Figure 7, indicating that the band ratio values were directly related to the concentrations of Hg^{2+} from 50 nM to 400 nM. Because the concentration of Hg^{2+} was higher than 400 nM, the band ratio values approached a maximum, indicating that the AuNPs were dispersed. After considering three times of the blank test standard deviations, the detection limit of Hg^{2+} was ca. 25 nM. Regarding the selectivity of the sensing system, several potential interference metal ions, including Zn^{2+}, Ca^{2+}, Co^{2+}, Ni^{3+}, Pb^{2+}, Fe^{3+}, and Cu^{2+}, were examined by applying the same condition, and the concentrations of the metal ions were all 100 times higher than that of Hg^{2+}. The calculated band ratio values at 525 and 750 nm in the presence of different metal ions are shown in Figure 8. Compared with Hg^{2+}, all of the metal ions showed no or considerably limited capabilities of anti-aggregation, suggesting the high selectivity toward Hg^{2+} of the proposed sensing system based on the dynamic anti-aggregation of gold nanocolloids. This result can be rationalized by the extremely high formation constant between l-penicillamine and Hg^{2+} than other examined metal ions.[59,63,64]

Analysis of Real Samples

To exam the feasibility of the sensing method proposed in this study for the detection of real samples, tap water samples were spiked with different concentrations of Hg^{2+} (100 nM to 400 nM) and the recovery values were 95.8 to 99.3% (see Table

S1 in the electronic supplement information). The good recoveries indicated that our system was capable for the detection of Hg^{2+} in real samples.

Conclusion

This study proposes a novel colorimetric sensing method based on the dynamic anti-aggregation of AuNPs for detecting mercury(II) ions in aqueous solutions. Compared with other applications, the proposed sensing method requires no surface modifications of AuNPs, thereby simplifying the sensing method procedures substantially. Furthermore, each measurement can be finished within 2 min while retaining the sufficient selectivity toward Hg^{2+}, thus increasing the utilities of the sensing method notably. Under optimal conditions, the sensitivity of the developed sensing method for detecting Hg^{2+} is ca. 25 nM.

Acknowledgments

The authors thank the Ministry of Science and Technology of Republic of China for financially supporting this work under Contract No. NSC100-2113-M-037-001-MY2 and NSC102-2113-M-037-014-MY2.

References

(1) Baughman, T. A. *Environ. Health Perspect.* **2006**, *114*, 147.

(2) Driscoll, C. T.; Mason, R. P.; Chan, H. M.; Jacob, D. J.; Pirrone, N. *Environ. Sci. Technol.* **2013**, *47*, 4967.

(3) Campbell, L.; Dixon, D. G.; Hecky, R. E. *J. Toxicol. Environ. Health, B* **2003**, *6*, 325.

(4) Morel, F. M. M.; Kraepiel, A. M. L.; Amyot, M. *Annu. Rev. Ecol. Evol. Syst.* **1998**, *29*, 543.

(5) Nolan, E. M.; Lippard, S. J. *Chem. Rev.* **2008**, *108*, 3443.

(6) Butler, O. T.; Cook, J. M.; Harrington, C. F.; Hill, S. J.; Rieuwerts, J.; Miles, D. L. *J. Anal. At. Spectrom.* **2006**, *21*, 217.

(7) Tao, S.; Gong, S.; Xu, L.; Fanguy, J. C. *Analyst* **2004**, *129*, 342.

(8) Tao, G.; N. Willie, S. *Analyst* **1998**, *123*, 1215.

(9) Torsi, G.; Desimoni, E.; Palmisano, F.; Sabbatini, L. *Analyst* **1982**, *107*, 96.

(10) White, W. W.; Murphy, P. J. *Anal. Chem.* **1977**, *49*, 255.

(11) Alder, J. F.; Hickman, D. A. *Anal. Chem.* **1977**, *49*, 336.

(12) Rofouei, M. K.; Rezaei, A.; Masteri-Farahani, M.; Khani, H. *Anal. Methods* **2012**, *4*, 959.

(13) dos Santos, V. C. G.; Grassi, M. T.; de Campos, M. S.; Peralta-Zamora, P. G.; Abate, G. *Analyst* **2012**, *137*, 4458.

(14) Arpadjan, S.; Vuchkova, L.; Kostadinova, E. *Analyst* **1997**, *122*, 243.

(15) Thompson, M.; Coles, B. J. *Analyst* **1984**, *109*, 529.

(16) Cope, M. J.; Kirkbright, G. F.; Burr, P. M. *Analyst* **1982**, *107*, 611.

(17) Ai, X.; Wang, Y.; Hou, X.; Yang, L.; Zheng, C.; Wu, L. *Analyst* **2013**, *138*, 3494.

(18) Gao, Y.; Yang, W.; Zheng, C.; Hou, X.; Wu, L. *J. Anal. At. Spectrom.* **2011**, *26*, 126.

(19) Sanchez-Rodas, D.; Corns, W. T.; Chen, B.; Stockwell, P. B. *J. Anal. At. Spectrom.* **2010**, *25*, 933.

(20) Leopold, K.; Foulkes, M.; Worsfold, P. J. *Anal. Chem.* **2009**, *81*, 3421.

(21) Rodrigues, J. L.; Alvarez, C. R.; Farinas, N. R.; Berzas Nevado, J. J.; Barbosa Jr, F.; Rodriguez Martin-Doimeadios, R. C. *J. Anal. At. Spectrom.* **2011**, *26*, 436.

(22) Park, C. J.; Do, H. *J. Anal. At. Spectrom.* **2008**, *23*, 997.

(23) Gong, J.; Zhou, T.; Song, D.; Zhang, L.; Hu, X. *Anal. Chem.* **2009**, *82*, 567.

(24) Liu, S.-J.; Nie, H.-G.; Jiang, J.-H.; Shen, G.-L.; Yu, R.-Q. *Anal. Chem.* **2009**, *81*, 5724.

(25) Jena, B. K.; Raj, C. R. *Anal. Chem.* **2008**, *80*, 4836.

(26) Jain, P. K.; Huang, X.; El-Sayed, I. H.; El-Sayed, M. A. *Acc. Chem. Res.* **2008**, *41*, 1578.

(27) Willets, K. A.; Van Duyne, R. P. *Annu. Rev. Phys. Chem.* **2007**, *58*, 267.
(28) Kim, Y.; Johnson, R. C.; Hupp, J. T. *Nano Lett.* **2001**, *1*, 165.
(29) Liu, X.; Atwater, M.; Wang, J.; Huo, Q. *Colloids Surf., B* **2007**, *58*, 3.
(30) Evanoff, D. D.; Chumanov, G. *J. Phys. Chem. B* **2004**, *108*, 13957.
(31) Saha, K.; Agasti, S. S.; Kim, C.; Li, X.; Rotello, V. M. *Chem. Rev.* **2012**, *112*, 2739.
(32) Ma, Y.; Jiang, L.; Mei, Y.; Song, R.; Tian, D.; Huang, H. *Analyst* **2013**, *138*, 5338.
(33) Chai, F.; Wang, C.; Wang, T.; Ma, Z.; Su, Z. *Nanotechnology* **2010**, *21*, 025501.
(34) Li, T.; Dong, S.; Wang, E. *Anal. Chem.* **2009**, *81*, 2144.
(35) Lin, C.-Y.; Yu, C.-J.; Lin, Y.-H.; Tseng, W.-L. *Anal. Chem.* **2010**, *82*, 6830.
(36) Yu, C.-J.; Tseng, W.-L. *Langmuir* **2008**, *24*, 12717.
(37) Ghosh, S. K.; Pal, T. *Chem. Rev.* **2007**, *107*, 4797.
(38) Daniel, M.-C.; Astruc, D. *Chem. Rev.* **2003**, *104*, 293.
(39) Lee, J. S.; Han, M. S.; Mirkin, C. A. *Angew. Chem. Int. Ed.* **2007**, *46*, 4093.
(40) Yu, C.-J.; Cheng, T.-L.; Tseng, W.-L. *Biosens. Bioelectron.* **2009**, *25*, 204.
(41) Duan, J.; Yang, M.; Lai, Y.; Yuan, J.; Zhan, J. *Anal.Chim. Acta* **2012**, *723*, 88.
(42) Chemnasiri, W.; Hernandez, F. E. *Sens. Actuators, B* **2012**, *173*, 322.
(43) Li, M.; Wang, Q.; Shi, X.; Hornak, L. A.; Wu, N. *Anal. Chem.* **2011**, *83*, 7061.
(44) Wang, H.; Wang, Y.; Jin, J.; Yang, R. *Anal. Chem.* **2008**, *80*, 9021.
(45) Huang, C.-C.; Yang, Z.; Lee, K.-H.; Chang, H.-T. *Angew. Chem. Int. Ed.* **2007**, *46*, 6824.
(46) Huang, C.-C.; Chang, H.-T. *Anal. Chem.* **2006**, *78*, 8332.
(47) Dubertret, B.; Calame, M.; Libchaber, A. J. *Nat. Biotechnol.* **2001**, *19*, 365.
(48) Ding, N.; Zhao, H.; Peng, W.; He, Y.; Zhou, Y.; Yuan, L.; Zhang, Y. *Colloids Surf., A* **2012**, *395*, 161.
(49) Lou, T.; Chen, L.; Zhang, C.; Kang, Q.; You, H.; Shen, D.; Chen, L. *Anal. Methods* **2012**, *4*, 488.
(50) Li, Y.; Wu, P.; Xu, H.; Zhang, Z.; Zhong, X. *Talanta* **2011**, *84*, 508.
(51) Lee, P. C.; Meisel, D. *J. Phys. Chem.* **1982**, *86*, 3391.
(52) Haiss, W.; Thanh, N. T. K.; Aveyard, J.; Fernig, D. G. *Anal. Chem.* **2007**, *79*, 4215.
(53) Link, S.; El-Sayed, M. A. *J. Phys. Chem. B* **1999**, *103*, 4212.
(54) Zakaria, H. M.; Shah, A.; Konieczny, M.; Hoffmann, J. A.; Nijdam, A. J.; Reeves, M. E. *Langmuir* **2013**, *29*, 7661.
(55) Basu, S.; Ghosh, S. K.; Kundu, S.; Panigrahi, S.; Praharaj, S.; Pande, S.; Jana, S.; Pal, T. *J. Colloid Interface Sci.* **2007**, *313*, 724.
(56) Glaspell, G. P.; Zuo, C.; Jagodzinski, P. W. *J. Cluster Sci.* **2005**, *16*, 39.
(57) Watanabe, S.; Seguchi, H.; Yoshida, K.; Kifune, K.; Tadaki, T.; Shiozaki, H. *Tetrahedron Lett.* **2005**, *46*, 8827.

(58) Lenz, G. R.; Martel, A. E. *Biochemistry* **1964**, *3*, 745.
(59) Kuchinskas, E. J.; Rosen, Y. *Arch. Biochem. Biophys.* **1962**, *97*, 370.
(60) Taladriz-Blanco, P.; Buurma, N. J.; Rodriguez-Lorenzo, L.; Perez-Juste, J.; Liz-Marzan, L. M.; Herves, P. *J. Mater. Chem.* **2011**, *21*, 16880.
(61) Ravichandran, M. *Chemosphere* **2004**, *55*, 319.
(62) Kornev, V. I.; Kardapol'tsev, A. A. *Russ J Coord Chem* **2008**, *34*, 896.
(63) Jalilehvand, F.; Leung, B. O.; Mah, V. *Inorg. Chem.* **2009**, *48*, 5758.
(64) Kõszegi-Szalai, H.; Paál, T. L. *Talanta* **1999**, *48*, 393.

Figure Captions

Scheme 1. Schematic diagram of the dynamic anti-aggregation phenomenon for the detection of Hg^{2+} proposed in this study.

Figure 1. (A) Extinction spectra of AuNPs colloidal solutions in the presence of (a.) 5 mM, (b.) 10 mM, (c.) 15 mM of chloride ion along with 2 μM of (—) l-penicillamine, (**.....**) l-glutathione, (------) l-cysteine methyl ester, l-cysteine (—•—•—), homocysteine (— — —), and l-methionine (—••—••); (d.), (e.), (f.) are the extinction spectra of AuNPs in the presence of 1 μM Hg^{2+} where the other conditions are the same as (a), (b), and (c), respectively. All the gold nanocolloids solutions contained 5 mM of citrate, the pH was 2.4, and the incubation time was 2 min. The particle concentration of gold nanocolloids was 2.85 nM.

(B) The absorbance ratio (Ex525/Ex750) of Aggregation agent-AuNPs versus Cl^- concentrations in the presence of 1 μM Hg^{2+}. Aggregation agent: 2 μM of (■) l-penicillamine, (●) l-cysteine, (▲) l-glutathione, (▼) l-methionine, (◆) l-cysteine methyl ester, (★) l-homocysteine. The hollow symbols corresponded to the same conditions but without Hg^{2+}. All the AuNPs solutions contained 5 mM of citrate, the pH was 2.4, and the incubation time was 2 min. The particle concentration of gold nanocolloids was 2.85 nM.

Figure 2. (A) The TEM image of l-penicillamine-AuNPs aggregates; (B) The TEM image of l-penicillamine-AuNPs aggregates in the presence of 1 μM Hg^{2+}. Both AuNPs solutions contained 2 μM of l-penicillamine, 10 mM of Cl^- and 5 mM of citrate where pH was 2.4.

Figure 3. The absorbance ratio (Ex525/Ex750) of AuNPs versus l-penicillamine concentrations in the presence (■) and in the absence of 1 μM Hg^{2+} (□).

The particle concentration of AuNPs wa 2.85 nM, the concentration of citrate buffer was 5 mM, the concentration of Cl^- was 10 mM, the pH was 2.4, and the incubation time was 2 min.

Figure 4. The absorbance ratio (Ex525/Ex750) of AuNPs versus solution pH in the presence (■) and in the absence of 1 μM Hg^{2+} (□). The particle concentration of gold nanocolloids was 2.85 nM, l-penicillamine concentration was 2 μM, the concentration of citrate buffer was 5 mM, the concentration of Cl^- was 10 mM, and the incubation time was 2 min.

Figure 5. (A) The absorbance ratio (Ex525/Ex750) of AuNPs in the presence (solid bar) and in the absence of 1 μM Hg^{2+} (hollow bar) using different buffer species. The particle concentration of gold nanocolloids was 2.85 nM, l-penicillamine concentration was 2 μM, the concentration of the examined buffer specie was 5 mM, the concentration of Cl^- was 10 mM, the pH was 2.4 and the incubation times was 2 min.

(B) The absorbance ratio (Ex525/Ex750) of AuNPs versus citrate concentration in the presence (■) and in the absence of 1 μM Hg^{2+} (□). The particle concentration of gold nanocolloids was 2.85 nM, l-penicillamine concentration was 2 μM, the concentration of Cl^- was 10 mM, the pH was 2.4 and the incubation times were 2 min.

Figure 6. The absorbance ratio (Ex525/Ex750) of AuNPs versus AuNPs particle concentration in the presence (■) and in the absence of 1 μM Hg^{2+} (□). The concentration of l-penicillamine was 2 μM, the concentration of citrate buffer was 5 mM, the concentration of Cl^- was 10 mM, the pH was 2.4 and the incubation time was 2 min.

Figure 7. The concentration profile of Hg^{2+} detected by the dynamic anti-aggregation method proposed in this study. The particle concentration of gold

nanocolloids was 2.85 nM, l-penicillamine concentration was 2 μM, the concentration of citrate buffer was 5 mM, the concentration of Cl^- was 10 mM, the concentration of citrate was 10 mM, the pH was 2.4, and the incubation time was 2 min. The inset shows the enlarged figure for the concentration under 400 nM.

Figure 8. The absorbance ratio (Ex525/Ex750) of AuNPs in the presence (solid bar) and in the absence of different metal ions (hollow bar). The concentration of Hg^{2+} was 1 μM and the concentrations of other examined metal ions were all 100 μM. The particle concentration of gold nanocolloids was 2.85 nM, l-penicillamine concentration was 2 μM, the concentration of citrate was 5 mM, the concentration of Cl^- was 10 mM, the pH was 2.4 and the incubation time was 2 min.

Scheme 1

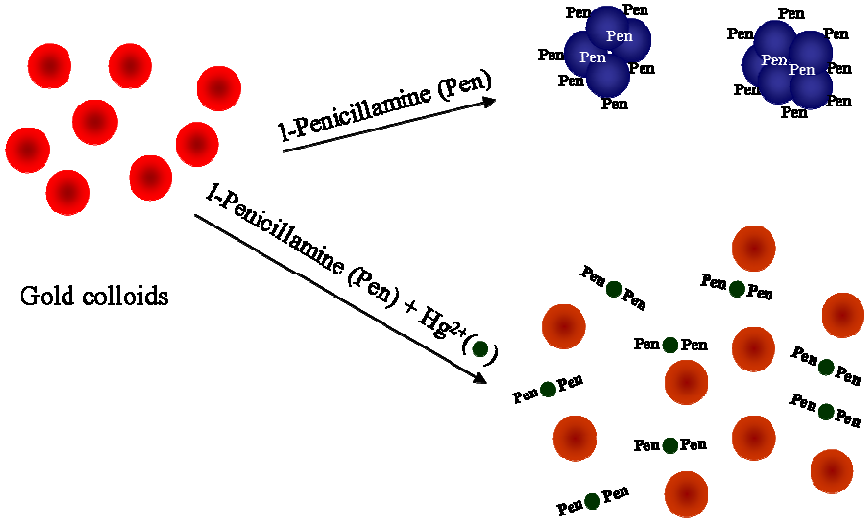

Figure 1A

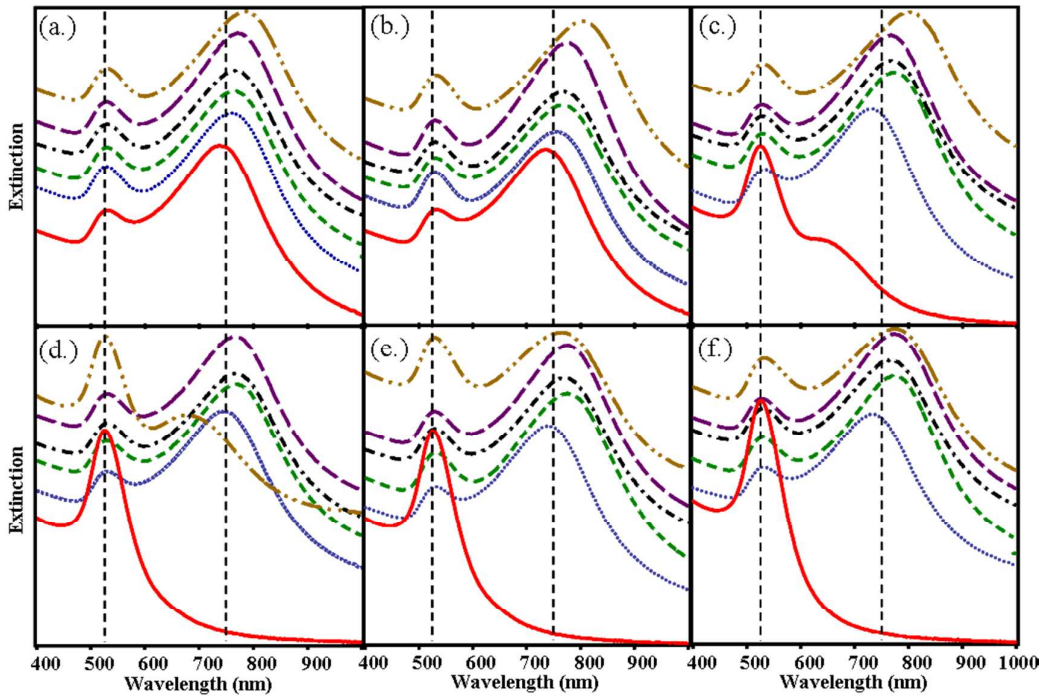

Figure 1B

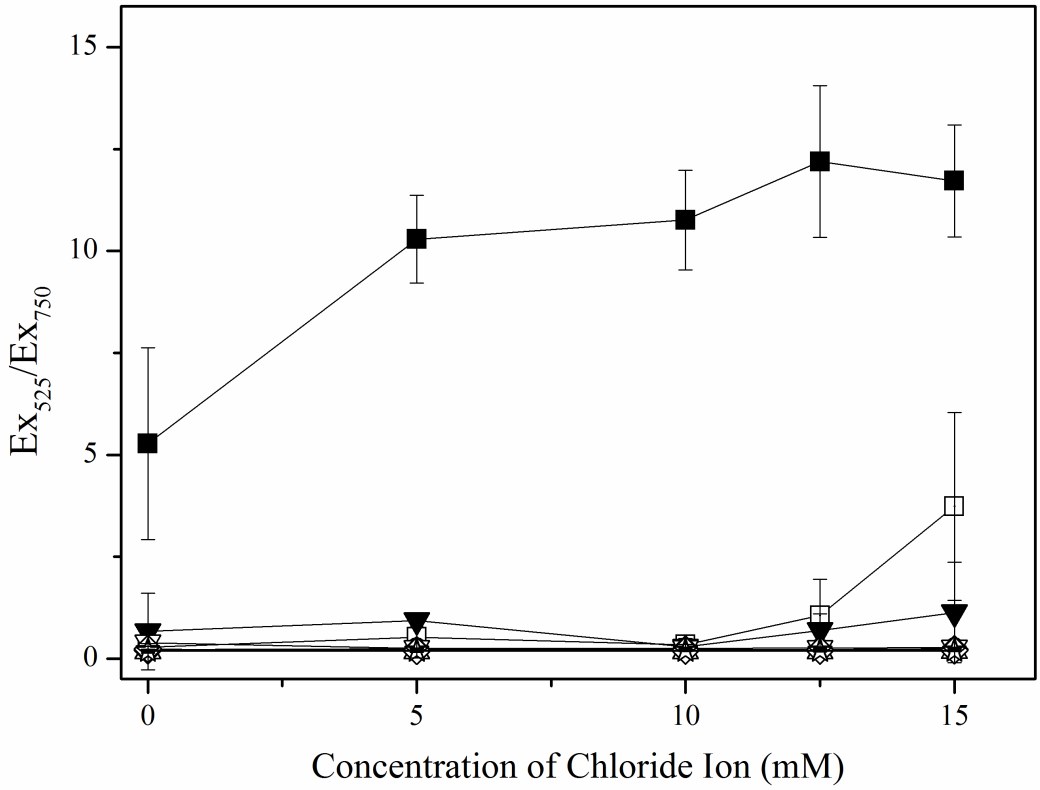

Figure 2

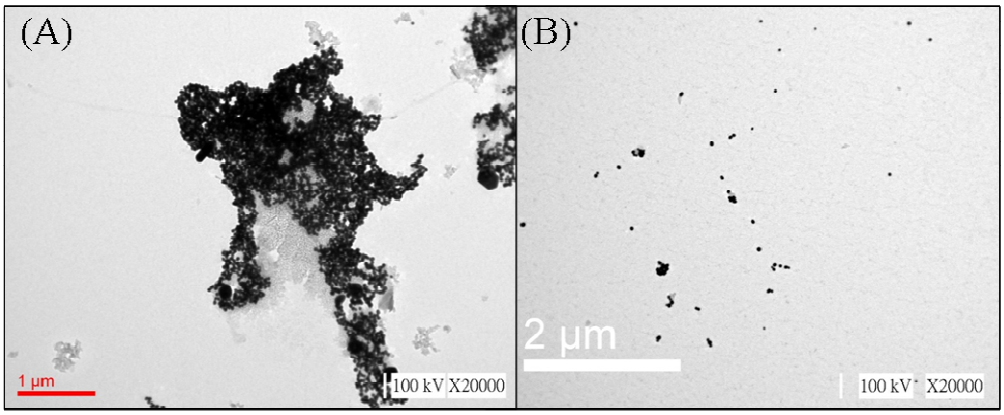

Figure 3

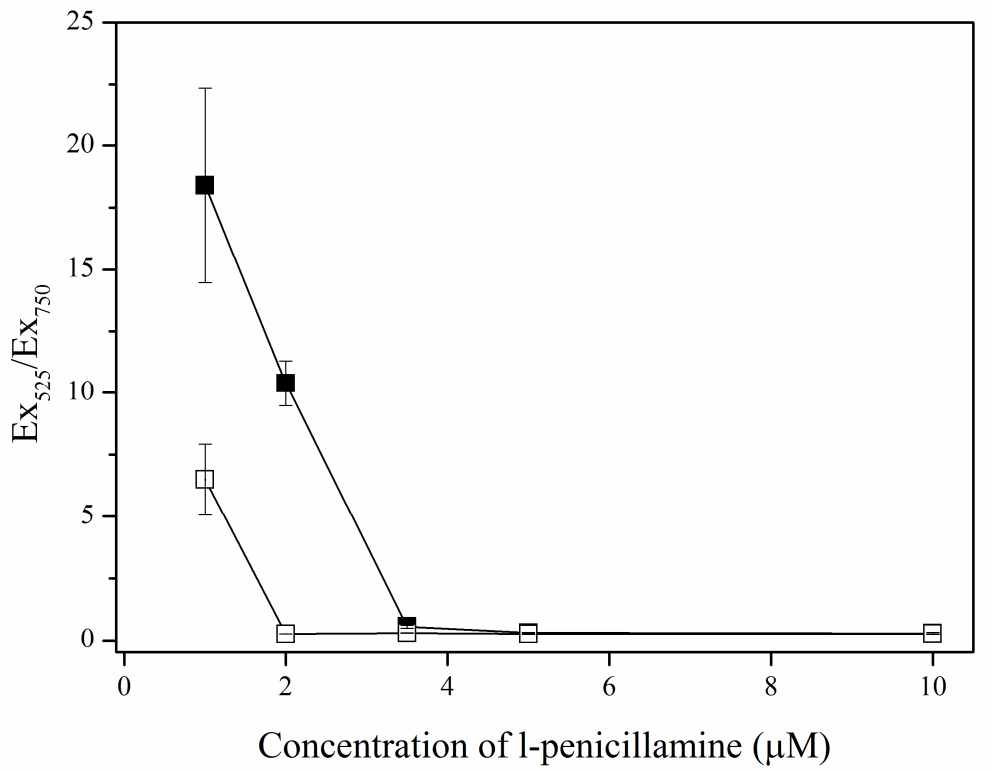

Figure 4

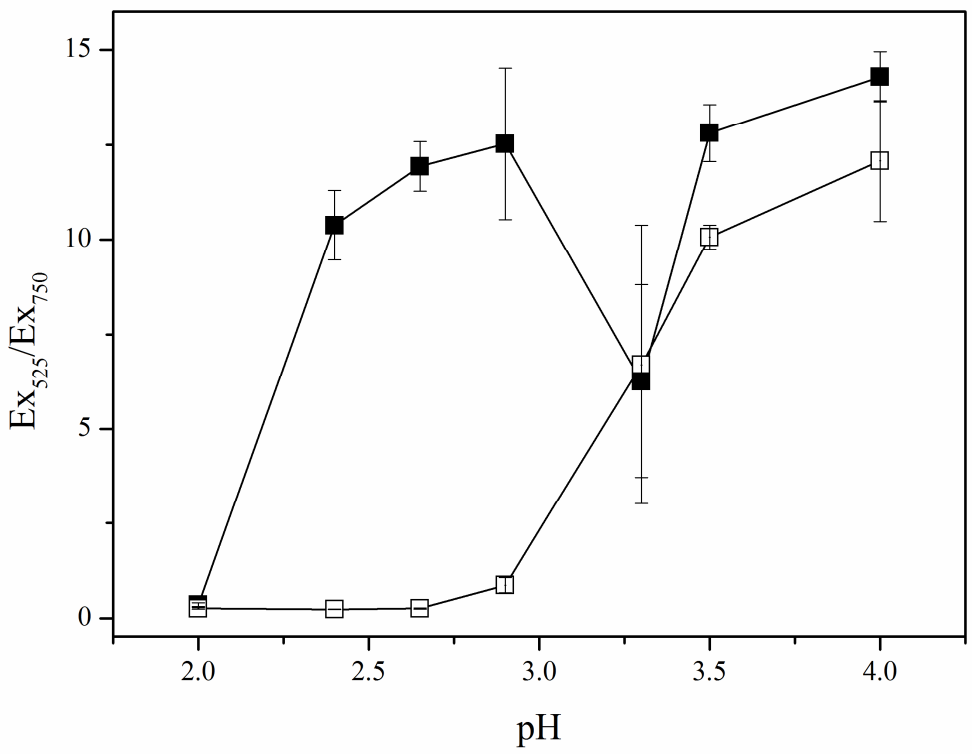

Figure 5A

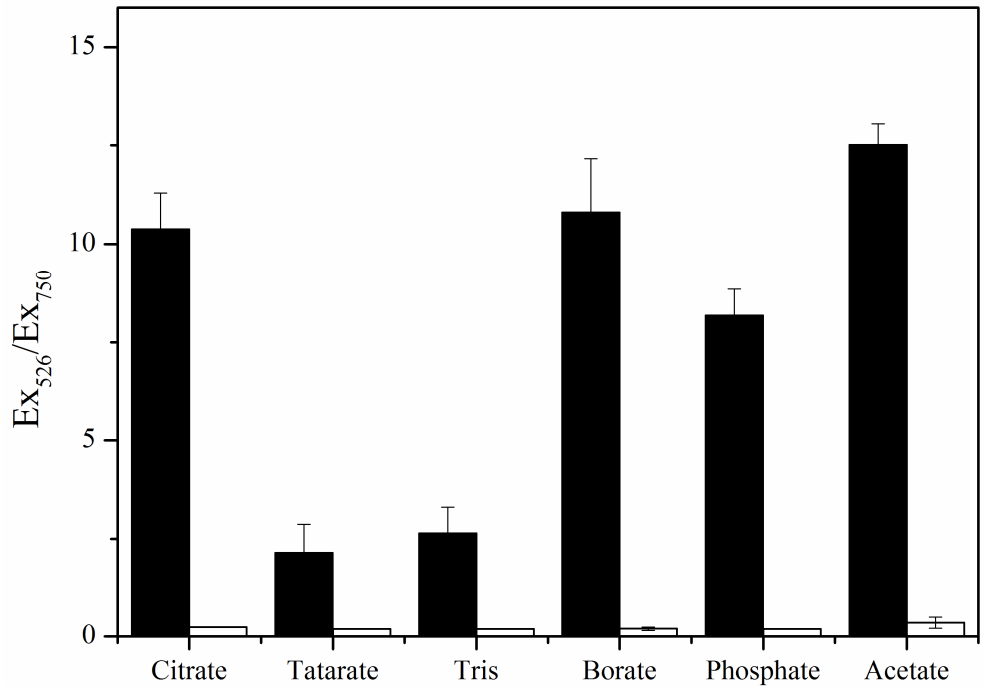

Figure 5B

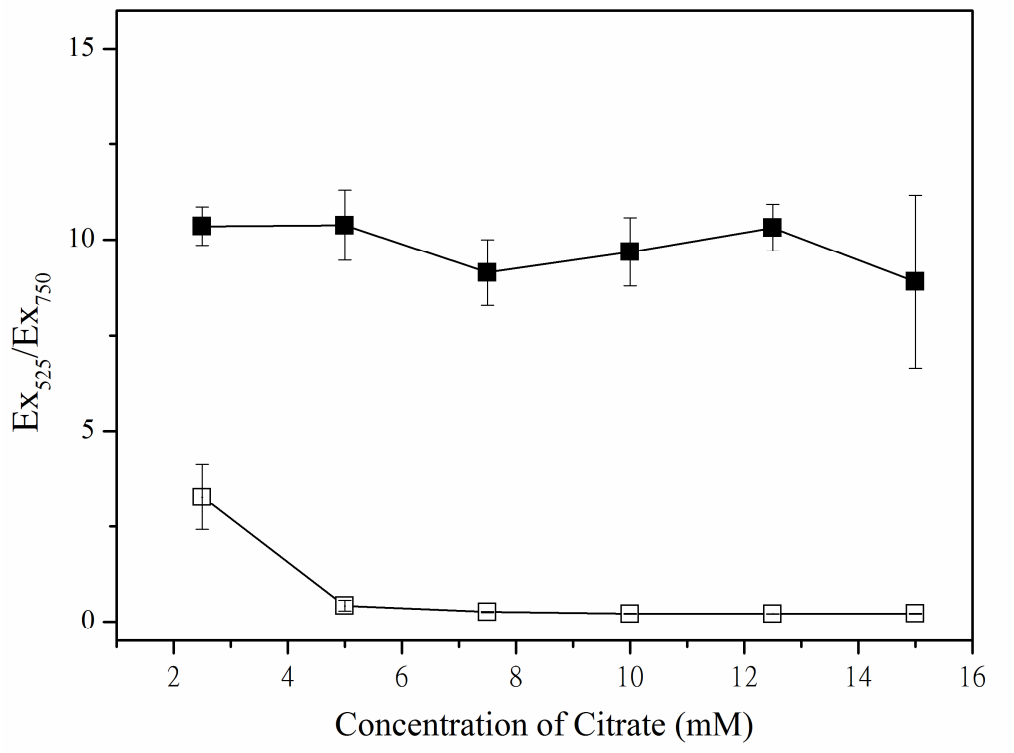

Figure 6

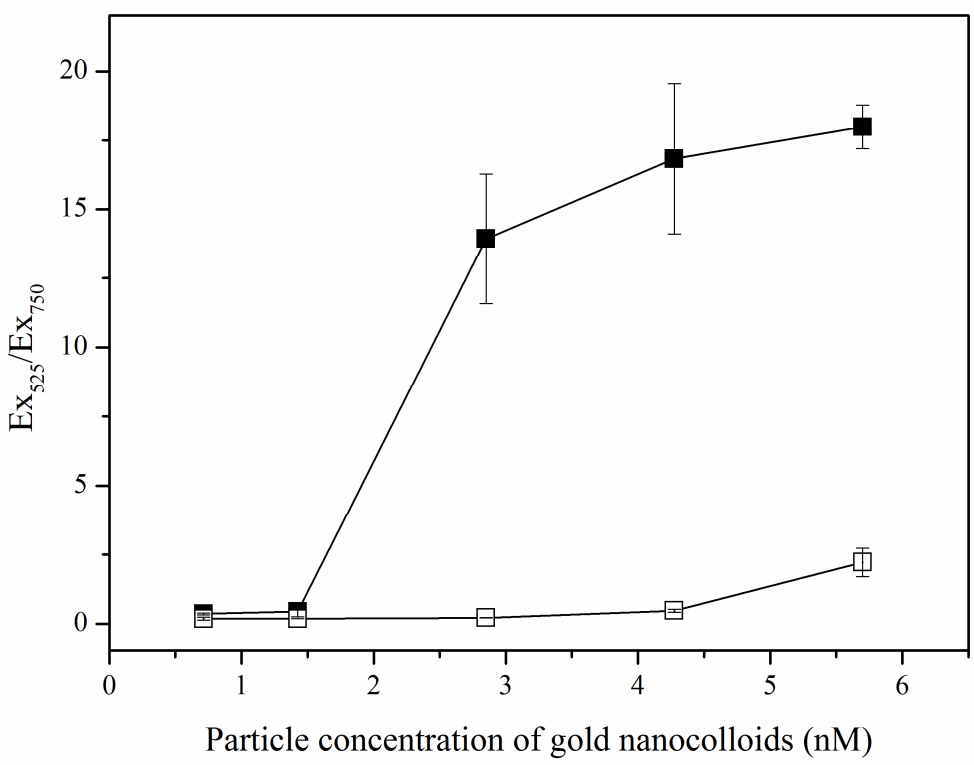

Figure 7

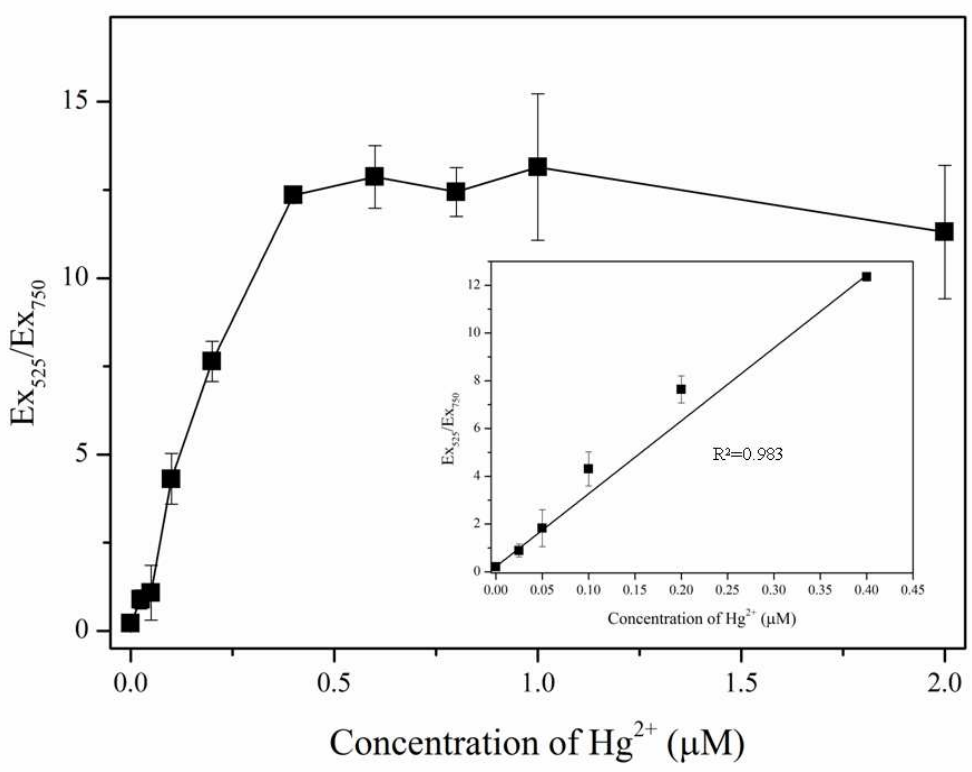

Figure 8